NURETH14-629

MODELLING OF SOLIDIFICATION EFFECT IN EULERIAN FUEL-COOLANT INTERACTION CODES

M. Uršič and M. Leskovar Jožef Stefan Institute, Ljubljana, Slovenia

Abstract

The solidification influence modeling in fuel-coolant interaction codes is strongly related to the modeling of the temperature profile inside the melt droplets and to the modeling of the mechanical effect of the formed crust on the fine fragmentation process. A purpose of the study was to enable solidification influence modeling in codes with an Eulerian formulation of the droplet field. Therefore additional transporte quantities based on the most important melt droplet features regarding the steam explosion phenomenon were derived. This enables a more accurate prediction of the amount of droplets participating in the fine fragmentation process during the explosion phase. Also the potential effect of the proposed modeling was assessed. The simulations supported the key role of the solidification in the steam explosion phenomenon.

Introduction

A steam explosion is a type of a fuel-coolant interaction (FCI), which results from the rapid and intense heat transfer that may follow the interaction between the molten material and the coolant [1]. The steam explosion phenomenon is divided into the premixing and the explosion phase. The premixing phase covers the interaction of the melt with the coolant prior the steam explosion. At the interaction the coolant vaporizes around the melt-coolant interface, creating a vapour film. The system may remain in the meta-stable state for a period ranging from a tenth of a second up to a few seconds. During this time the jet is fragmented into the melt droplets of the order of several mm in diameter, which may be further fragmented by the coarse break up process into melt droplets of the order of mm in diameter. If during the meta-stable state a local vapour film destabilization occurs, then the steam explosion may be triggered due to the melt-coolant contact. The destabilization causes the fine fragmentation of the melt droplets into fragments of the order of some 10 µm in diameter. The fine fragmentation process rapidly increases the melt surface area, vaporizing more coolant and increasing the local vapour pressure. This fast vapour formation due to the fine fragmentation spatially propagates throughout the melt-coolant mixture causing the whole region to become pressurized by the coolant vapour. Subsequently, the high pressure region behind the propagation front expands and performs work on its surrounding. The time scale for the steam explosion phase itself is in the order of ms.

Steam explosion experiments have revealed important differences in behaviour among melts [2]. For example the steam explosion experiments performed in the KROTOS facility have revealed important differences in behaviour between the alumina and the corium melts [3-5]. As seen in Figure 1, the energy conversion efficiency (defined as the ratio between the kinetic energy after the explosion and the initial thermal energy of the melt) for the corium melt (80wt% UO₂ and 20wt% ZrO₂) is significantly lower than for the alumina melt (Al₂O₃). The differences in the physical material properties are one of the probable reasons for the observed important differences in the efficiency [6]. The differences in the material properties are causing differences in the melt jet break

up, the melt solidification and the void production during the premixing phase. The crust formation is believed to be one of the most decisive consequences of the material properties regarding the limitation of the steam explosion strength. The crust inhibits the fine fragmentation process of the melt droplets during the explosion phase and if the crust is thick enough it completely prevents it. The crust formation during the premixing phase in combination with the void production and the jet break up could explain the observed differences in the explosion energy conversion efficiency between the alumina and the corium melts.

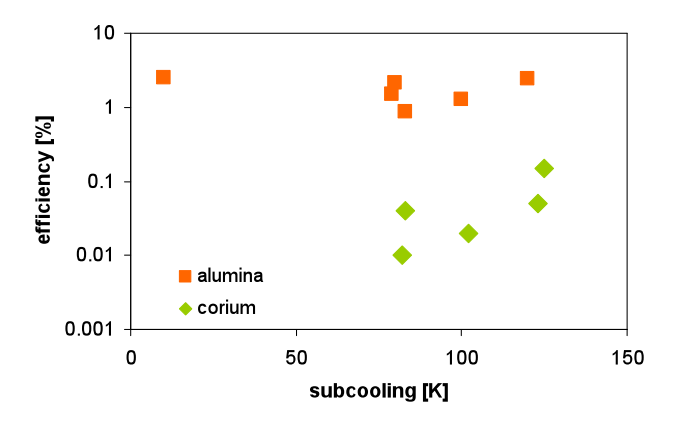


Figure 1 Steam explosion energy conversion efficiency as a function of water sub-cooling for KROTOS experiments [3-5].

Although it is believed that in reality the temperature profile inside a melt droplet is not flat, FCI codes in general consider homogeneous cooling of the melt droplets. Thus the crust formation is not taken into account in enough detail to be able to predict adequately the solidification effects on FCI. Consequently, such FCI codes are not able to predict the observed differences in the explosion energy conversion efficiency among different melt materials. Recently, due to the recognized importance of the solidification issue, new solidification influence models are being developed and implemented into FCI codes [7-10]. The purpose of the solidification influence modelling is to improve the determination of the melt droplet mass, which can be efficiently fine fragmented in the steam explosion process. Furthermore, the modelling enables an improved determination of the void, which is an additional limiting process in the steam explosion phenomenon.

The aim of the study was therefore to develop an improved solidification influence modelling (ISIM) and an approach for its integration into the Eulerian FCI codes. The aim was also to asses the potential effect of the developed ISIM approach on the simulation results.

1. Improved solidification influence modelling

The solidification influence modelling is strongly related to the modelling of the temperature profile inside the melt droplet and to the computation of the mechanical effect of the crust thickness on the fragmentation process [10]. The purpose of the temperature profile modelling is to improve the knowledge about the melt droplet crust thickness and the surface temperature. The surface temperature defines the heat flux from the droplet to the surrounding and it is therefore influencing directly important FCI parameters, as the crust formation and the void fraction. Further, the presence of the crust influences the ability of the droplet to fragment already before the droplet is significantly solidified. The comparative review of the FCI codes showed that none of the codes is computing the mechanical effect of the solid layer on the fragmentation [8].

1.1 Temperature profile modelling

The melt droplet quenching depends on the processes of heat transfer inside the melt droplet and from the droplet to the surrounding [10,11]. A typical droplet in the FCI experiments may be considered to be cooled by thermal radiation only from its surface (i.e. opaque). In the mathematical-physical model it was considered that the heat transfer among the droplets is insignificant as compared to the local heat transfer from individual droplets and that the heat transfer inside the melt droplet is by heat conduction only. Also, it was assumed that the materials are eutectic and that the material properties are constant.

By solving the equations of the mathematical-physical model, the temperature profile may be calculated. Analytical solutions exist only for specific initial and boundary conditions, which in general do not represent situations during the FCI phenomena. On the other hand a direct numerical solution of the model would increase the computational requirements of FCI codes too much. Therefore, it was suggested to apply the heat transfer model for the opaque droplets (HTMOD) approach [10]. In the HTMOD approach, the temperature profiles in central, boundary and crust droplet layers are prescribed:

$$T_{l}[r,t] = \begin{cases} T_{cen}[t] & ; \quad r \leq R - \delta_{s}[t] - \delta_{l}[t] \\ T_{cen}[t] - \frac{T_{cen}[t] - T_{int}[t]}{\delta_{l}[t]} \cdot (r - R + \delta_{s}[t] + \delta_{l}[t])^{2} & ; \quad R - \delta_{s}[t] - \delta_{l}[t] < r \leq R - \delta_{s}[t] \end{cases}$$

$$T_{s}[r,t] = \begin{cases} T_{m} + \frac{T_{sur}[t] - T_{m}}{\delta_{s}[t]} (r - R + \delta_{s}[t]) & ; \quad R - \delta_{s}[t] < r \leq R \end{cases}$$

$$T_{cen}[t] - \frac{T_{cen}[t] - T_{sur}[t]}{R^{2}} r^{2} & ; \quad r \leq R \wedge \delta_{s}[t] = R \end{cases}$$

$$T_{cen}[t] = \begin{cases} T_{0} & ; \quad \delta_{l}[t] \neq R - \delta_{s}[t] \\ T_{cen}[t] & ; \quad \delta_{l}[t] = R - \delta_{s}[t] \end{cases}$$

$$T_{int}[t] = \begin{cases} T_{sur}[t] & ; \quad \delta_{s}[t] = 0 \\ T_{m} & ; \quad \delta_{s}[t] \neq 0 \end{cases}$$

where T_{cen} is the central temperature and T_{int} is the temperature between the boundary δ_l and the crust δ_s layer, i.e. T_m (if the crust layer is present) or the droplet surface temperature T_{sur} (if the crust layer is absent). T_0 is initial temperature and R is droplet radius. Obviously, the temperature profiles are in general a function of four HTMOD parameters: the surface temperature T_{sur} , the central temperature T_{cen} , the crust layer thickness δ_s and the boundary layer thickness δ_l . To calculate the time development of these parameters the mathematically closed system of equations (heat balance equation and transient equation for the determination of the solid crust growth) with prescribed initial (the initial droplet temperature) and boundary conditions (the boundary condition for the temperature profile gradient, which has to result in a heat flux equal to the surface heat flux) is used.

A similar approach, based on the parabolic temperature profile assumption in the boundary layer, is also applied in the JASMINE and JEMI FCI codes [9,12]. The model in the JEMI code uses additionally the linear temperature profile in the crust layer. The linear temperature profile in the crust layer is also implemented in the VAPEX code [7]. In the JASMINE code, the effect of the crust on the fragmentation is not considered, therefore the crust layer is not modelled [8]. Also PM-ALPHA uses non-homogenous profiles [8].

The HTMOD approach was validated on an accurate finite differences solution of the mathematical-physical model [10]. A qualitatively and quantitatively good agreement was achieved.

1.2 Fragmentation criterion

The steam explosion energy conversion efficiency depends on the melt droplet mass, which can be rapidly fine fragmented during the explosion process. The fine fragmentation occurs essentially due to the velocity difference between the melt droplets and the surrounding media. Experiments revealed that not only liquid droplets but also partly solidified droplets can participate in the fine fragmentation process [13].

The ability of a melt droplet to undergo fragmentation depends on its surface conditions. For liquid droplets the surface tension is acting to retain the droplets form under the presence of hydrodynamic forces. For liquid droplets the standard Weber number is commonly used to characterize the ability of a droplet to be fragmented due to hydrodynamic forces:

$$We = \frac{\rho_c v_{rel}^2 D}{\sigma},\tag{2}$$

where ρ_c is the coolant density, v_{rel} is the relative velocity between the droplet and the coolant, D is the diameter of the droplet and \bullet is the surface tension. Once a crust is created on the droplet surface, the role of the surface tension is replaced by the stabilizing force of the crust. The application of the standard Weber number can be therefore extended beyond completely liquid conditions to generalize its use for characterizing the droplet fragmentation by relative flows.

For the determination of conditions, when the relative flow is sufficient to fragment a droplet with a crust, a criterion based on the definition of the standard Weber number was proposed [10]. The criterion compares the effects of hydrodynamic forces and the crust stiffness, which stabilizes the crust. For a crust thickness, which is significantly lower as compared with the melt droplet diameter, the thin plate approximation can be used to assess the mechanical effects in these conditions. Therefore the crust stiffness:

$$D_{s} = \frac{1}{12} \frac{E\delta^{3}}{1 - \mu^{2}},\tag{3}$$

which assumes elastic behaviour of the thin crust, is proposed to define the corresponding modified Weber number:

$$We^* = \frac{\rho_{\epsilon} v_{rel}^2 D^3}{E \delta_{\epsilon}^3} \left(-\mu^2 \right) \tag{4}$$

The crust stiffness depends on the crust thickness δ_s , Young modulus E and Poisson ratio μ .

It is assumed that the use of the proposed modified Weber number as a criterion is appropriate for steam explosion simulations, because the final limitation of the fragmentation presumably occurs already for small relative crust thicknesses [14]. Based on the experimental results [13] the critical modified Weber number for fine fragmentation is estimated to be between 1 and 5 [10].

2. Solidification modelling in energetic Eulerian FCI codes

The implementation of the solidification influence modelling in FCI codes depends on how the melt droplets are described. Generally, the melt droplets are described either with the Lagrangean or the Eularian simplification.

In FCI codes, where the droplets treatment is Lagrangean, the required information is obtained by tracking directly the representative melt droplet groups. Each group has its own specific properties (e.g. velocity, crust thickness, temperature). ISIM is therefore directly applicable in all Lagrangean FCI codes.

With the Eulerian formulation the melt droplets are treated as a phase, which is homogenously distributed in each computational cell. Due to the inflow and outflow of the droplet phase in the computational cells, droplets with different properties are mixed. Droplets with average properties are thus present in each cell. The average droplet property values (e.g. surface temperature, crust thickness, surface area) have to be reconstructed in space and time. For the reconstruction the value of quantities which are calculated by the corresponding balance and the transport equations must be known.

2.1 Transport quantities

In ISIM, the HTMOD approach is used to define the conditions inside the melt droplets. For the reconstruction of the four HTMOD parameters and the droplet radius, a mathematically closed system of relations and conditions has to be defined and solved. Considering that the temperature in the droplet can not exceed the initial melt temperature (i.e. initial condition), four relations are necessary for the reconstruction. In those relations the balance and the transport quantities are linked to the HTMOD parameters and the droplet radius. Two quantities are usually obtained within the standard Eulerian approach, i.e. the internal droplet energy and the droplet surface area. Two additional transport quantities are required to close the system of relations.

The introduced additional transport quantities should represent the most important melt droplet features regarding the FCI modelling to get the best results. It was considered that the appropriate determination of the steam explosion strength is the most important goal of the FCI codes when simulating energetic FCI [10]. The strength of the steam explosion depends on the mass of melt droplets, which can efficiently participate in the steam explosion that is the mass of droplets capable to undergo fine fragmentation in regions with enough water available for vaporization and for enabling the fine fragmentation process. Evidently, the introduced transport quantities are most appropriately defined if they improve the prediction of the melt droplets capability to be fine fragmented and the prediction of the void fraction.

2.1.1 Ability to fragment

As discussed in Section 1.2, the capability of partly solidified droplets to undergo the fine fragmentation may be assessed with the modified Weber number. The modified Weber number considers the crust stiffness as a stabilizing force acting to retain the crust under the presence of hydrodynamic forces. Thus, one can consider the crust stiffness to be an important fundamental melt droplet property. The first transport quantity was therefore defined based on the crust stiffness definition given in Eq. (3):

The 14th International Topical Meeting on Nuclear Reactor Thermalhydraulics, NURETH-14 Toronto, Ontario, Canada, September 25-30, 2011

$$\Phi_{\delta} = \frac{6}{\pi} \alpha_d \left(\frac{\delta_s}{D}\right)^3, \tag{5}$$

where α_d is the droplet volume fraction. The ability to fragment is the highest when the transport quantity equals zero.

2.1.2 Average cooling rate

In FCI modelling the proper determination of the heat transfer between the melt droplet and its surrounding is crucial. The heat transfer depends on the droplet surface area, the droplet surface temperature and the conditions in the droplet surrounding. The conditions on the droplet surface, which vary with time, are conducted inside the droplet. Consequently, the temperature profile reflects the history of the droplet cooling. With the HTMOD approach, the temperature profiles are pre-described. With such an approach, the gradient of the temperature profile at the droplet surface represent a measure of the average heat flux between the melt droplet and its surrounding in the recent period. The temperature gradient at the droplet surface therefore contains information about the droplets cooling and was used for the second transport quantity definition:

$$\Phi_T = 6 \frac{\alpha_d}{D} \left(-\lambda \frac{\partial T}{\partial r} \Big|_{r=R} \right), \tag{6}$$

where λ is the thermal conductivity. A favourable property of the second transport quantity is that it enables a stable reconstruction of the surface temperature and reflects the droplet recent cooling history. The improved surface temperature prediction also improves the prediction of the void fraction.

2.2 Transport equations

The solution of the additional transport equations in FCI codes is discussed separately for the premixing and the explosion phase. The premixing phase lasts from a tenth of a second up to a few seconds, whereas the explosion phase itself lasts only about a few ms. The main processes of interest are also different during the premixing and the explosion phase. In the premixing phase the melt droplet generation during the jet fragmentation process, the droplet quenching, the droplet fragmentation and the potential droplet disappearance during the coalescence process are followed. But during the explosion phase the fine fragmentation, which rapidly increases the melt surface area and consequently the heat transfer from the fragments to water, is the dominant process of interest.

2.2.1 <u>Premixing phase</u>

The corresponding transport equations for both introduced transport quantities are:

$$\frac{\partial \Phi_{\delta}}{\partial t} + \nabla (\Phi_{\delta} \mathbf{v_d}) = \Gamma_{\delta}^{q} + \Gamma_{\delta}^{j} + \Gamma_{\delta}^{e} + \Gamma_{\delta}^{f},
\frac{\partial \Phi_{T}}{\partial t} + \nabla (\Phi_{T} \mathbf{v_d}) = \Gamma_{T}^{q} + \Gamma_{T}^{j} + \Gamma_{T}^{e} + \Gamma_{T}^{f},$$
(7)

where v_d is the droplet velocity field. The right-hand side of the equations represents the source terms and must be further specified. The droplet quenching source term Γ^q model considers the cooling of the droplet due to the heat transfer. The quenching influences the temperature profile

inside the droplet and is defined with the HTMOD approach. With the jet fragmentation new melt droplets are being formed from the jet. In the jet fragmentation source term Γ^j model, it was assumed that new born liquid droplets are well mixed and therefore have a flat temperature profile. Coalescence occurs when melt droplets interact among themselves or with the continuous jet field. It was assumed in the coalescence source term Γ^c model that droplet coalescence is not allowed if a crust is present on the droplet surface. The melt droplet fragmentation process occurs once the criterion for fragmentation is satisfied. The use of the ordinary and modified Weber numbers was considered to be suitable for the fragmentation criterion of the completely liquid and partly solidified droplets respectively. In the fragmentation source term Γ^f model it was considered that the fragments created during the fragmentation process are still big enough to be considered as droplets and the temperature profile changes proportionally to the change of the droplet size (i.e. stiffness is not affected).

2.2.2 Explosion phase

The duration of the explosion phase is too short to influence importantly the temperature profile inside the melt droplets. Therefore, the development of the temperature profile during the explosion phase was not modelled. However information about the droplet ability to fragment is crucial for the proper determination of the mass transfer between droplets and fine fragments. Consequently, only the introduced transport quantity named ability to fragment (Section 2.1.1) defined during the premixing phase is calculated by the corresponding transport equation:

$$\frac{\partial \Phi_{\delta}}{\partial t} + \nabla (\Phi_{\delta} \mathbf{v_d}) = \Gamma_{\delta}^{ff}, \tag{8}$$

where now in the source term the fine fragmentation of the droplet is taken into account. In the source term model it was considered that the fine fragments originate only from the surface layer of the droplet (i.e. stripping). The temperature of the fine fragments is equal to the melt droplet bulk temperature. The effect of the crust thickness on the fine fragmentation process is calculated with the modified Weber number, whereas for liquid droplets the standard Weber number criterion is used.

2.3 Reconstruction algorithm

In the Eulerian FCI codes, the reconstruction of the melt droplets conditions is necessary due to the inherent averaging in computational cells caused by the convection terms and by the source terms (e.g. jet fragmentation). The four HTMOD parameters (T_{sur} , T_{cen} , δ_s , δ_l) and the droplet size must be defined in each computational cell during each time step.

For the reconstruction, a mathematically closed system of relations and conditions must be set with the following calculated quantities: the standard Eulerian FCI code quantities of the internal droplet energy and the interfacial area, the introduced transport quantities named ability to fragment Φ_{δ} and average cooling rate Φ_{T} , and the initial melt temperature. The melt droplet surface area is used to define the droplet size. The crust thickness, which reflects the droplet ability to undergo the fine fragmentation, is determined from Φ_{δ} . The gradient of the temperature profile on the droplet surface reflects the recent cooling history and it is determined from Φ_{T} . Finally, the HTMOD parameters are analytically calculated in a way that the reconstructed HTMOD parameters also satisfy the droplet internal energy and initial condition.

When droplets exposed to similar histories are mixed the reconstructed HTMOD parameters are used. But, when mixing of droplets with significantly different histories occurs, a flat temperature profile as the first averaging approximation is conservatively prescribed and the crust thickness is determined based on the internal droplet energy.

3. Global potential effect in energetic FCI

The physically-based ISIM enables a more accurate determination of the melt droplet surface conditions which drive the heat transfer during the premixing phase and determine the droplet ability to undergo the fine fragmentation during the explosion phase. Therefore the developed ISIM was implemented in the exploring version of the MC3D code and was used to asses the potential effect of solidification on the simulation results.

3.1 Implementation to exploring version of MC3D code

The MC3D code is a multi-dimensional Eulerian code devoted to study multi-phase and multi-constituent flows in the field of nuclear safety [15]. In the standard MC3D solidification influence model the melt droplets solidification influence is taken into account by the comparison of the melt droplets bulk temperature with the melt solidification temperature. If the melt droplets bulk temperature is higher than the melting temperature the melt droplets are treated as liquid, allowing droplets fragmentation. Since it is believed that in reality the temperature profile inside a melt droplet is not flat, the ISIM approach was implemented into the MC3D code, version 3.6.1 [10]. The MC3D code with the implemented ISIM approach was declared as the exploring version of MC3D.

The implementation of ISIM into the exploring version of MC3D required an additional verification and validation. The validation and verification was done in three steps, which cover numerical, reconstruction algorithm capability and physical tests [16]. With the performed numerical tests, it was verified that the HTMOD approach and the assumptions used to define the source terms are appropriately implemented. In addition, the ability of the convective terms to transport properly the introduced transport quantities was validated. With the reconstruction capability tests, the successful reconstruction of the melt droplet properties, when droplets with similar temperature profiles are mixing, was verified. In case that the reconstruction is unsuccessful, which may happen if the temperature profiles of mixed droplets are too different, the flat temperature profile approximation is applied. The problem of the occasionally unsuccessful temperature profile reconstruction could be minimized by introducing groups of particles, which would reduce the possibility of mixing droplets with significantly different cooling histories. The proper implementation of the fragmentation criterion, which is based on the modified Weber number, was verified in the physical tests.

3.2 Assessment to potential effect

3.2.1 Simulation

Three parallel simulations were performed to demonstrate the potential effect of ISIM on the calculation results. The simulations were performed with and without considering solidification (i.e. no solid). Solidification was considered with the use of the standard solidification model (i.e. standard) and with the use of the improved solidification model (i.e. ISIM).

As seen in Figure 2, a simplified 2D geometry was used for simulation. The mesh was axial symmetrical and the cylindrical coordinates were used. The radius of the mesh was 0.223 m and the height was 1.68 m. Based on the convergence analysis results the mesh size of 20x80 cells was chosen. The typical cell dimension in the test section was 7x20 mm².

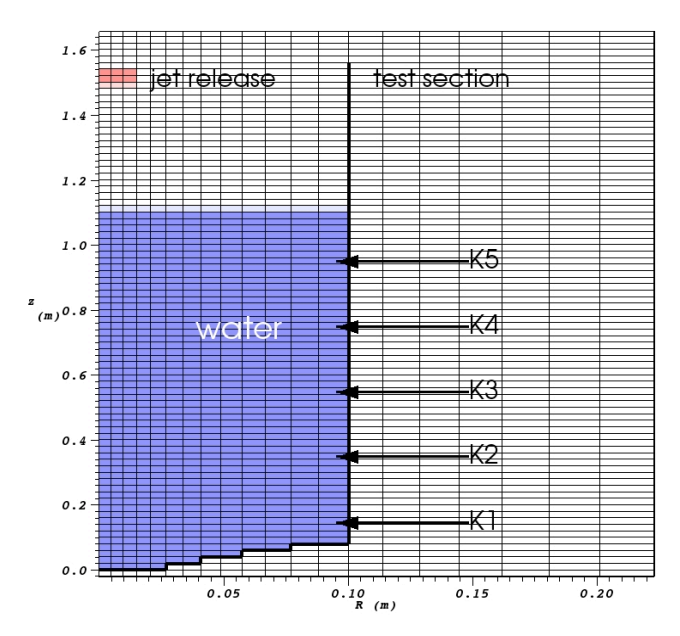


Figure 2 The geometry of the computational model consisting of 20x84 cells.

The melt release location in the premixing phase was set at 1.54 m. The diameter of the release was 0.03 m and the initial jet release velocity was set to 1.5 m/s. The fragmentation of the jet into droplets during the premixing phase was modelled with the global model [8,15]. The size of the droplets created by the jet fragmentation was set to 2 mm. Secondary break up of the melt droplets was not considered; therefore the generated droplet size during the jet fragmentation was also the final size of the droplets. The creation of non-condensable hydrogen during the interaction of corium with water vapour was also not modelled.

The premixing phase was simulated for a period of 1 s. The explosion phase was simulated for a period of 10 ms. The triggering was activated at the time of the melt-bottom contact.

3.2.2 Results

The strength of the steam explosion depends on the mass of melt droplets, which can efficiently participate in the steam explosion that is the mass of droplets being capable to undergo fine fragmentation in regions with enough water available for vaporization and for enabling the fine fragmentation process (hereafter denoted as available mass).

In Figure 3 (left) the results are shown for the performed premixing phase simulations. The ISIM mass in figure is shown for crust thickness smaller than 200 μ m, because steam explosion experiments with single droplets of iron oxide revealed that melt droplets may typically not undergo fine fragmentation if the formed solid crust is thicker than ~10%-20% of the droplet radius [18]. The results show a significant decrease of the available mass due to the strong effect of solidification. In the simulations, the ISIM results show an additional decrease of the available mass if compared with the standard results. In Figure 4 the spatial distribution of melt droplets and their level of

solidification at triggering time is shown for the ISIM results. As seen in the figure, only a small fraction of droplets is still liquid at triggering time.

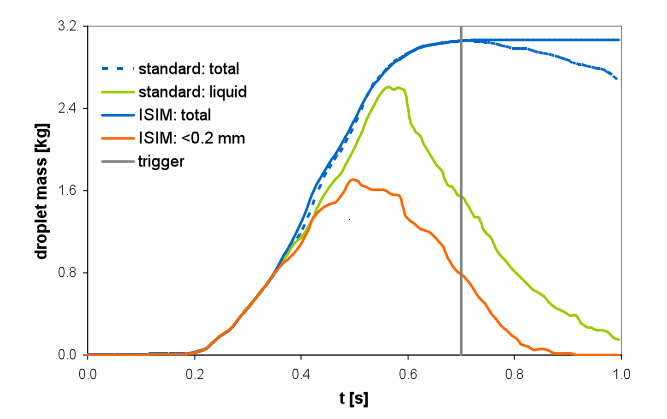
In Figure 3 (right) the calculated pressure loads at the location K4 (see Figure 2) are given for the performed explosion phase simulations. The ISIM simulation with the critical modified Weber number set to 3 predicts a significant reduction of the pressure loads if compared with the standard results and especially if compared with the results when the solidification is not considered at all. If the efficiency evaluation is made with the assumption that the water slug above the explosion point is accelerated upward transforming the impulse into kinetic energy, then the efficiency for ISIM in regard to the no solid case was reduced by one order of magnitude. As seen in Figure 3 (left), for the ISIM calculations the available mass for fine fragmentation is significantly lower if compared to the standard calculations and even lower if compared to the total mass available when no melt solidification is considered. Consequently the loads are lower.

The purpose of the simulations was to justify that melt solidification may significantly reduce the steam explosion strength and that consequently the solidification influence has to be adequately modelled, on a sufficient high level and on a physically sound basis to enable a reliable extrapolation of experimental findings to reactor conditions.

4. Conclusions

The paper presents a contribution to physically-based solidification influence modelling in the Eulerian FCI codes. It also examines the effect that the choice of the solidification modelling approach has on the simulation results of complex steam explosion experiments.

In the paper a physically-based ISIM was introduced. ISIM is reasonably complex to consider adequately the effect of the melt material properties, but still simple enough to be applicable for the implementation into FCI codes. The temperature profile modelling provides the improved information about the most important droplet parameters – the crust formation and the surface temperature. The implication of the improved surface temperature knowledge into the heat transfer modelling improves the prediction of the void production during the premixing phase. Further, the implication of the improved crust thickness knowledge into the mass transfer modelling enables the prediction of the droplet mass, which can be fine fragmented during the explosion phase. To enable the modelling of the mass transfer the modified Weber number was introduced.



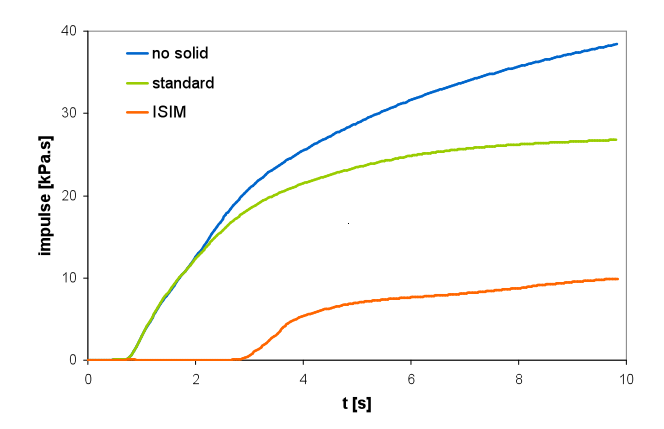


Figure 3 Premixing results on left shows total droplet mass, mass of liquid droplets for standard simulations and mass of melt droplets with a crust below 200 µm. Explosion results on right shows

comparison of calculated pressure impulses solidification was not considered (no solid) and when it was taken into account (i.e. standard and ISIM approach).

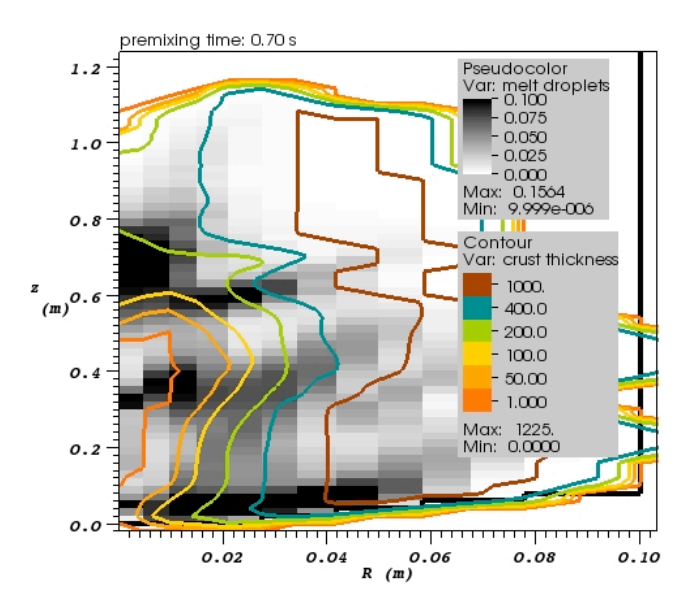


Figure 4 Distribution of melt droplets (field) and crust thickness in µm (contour) for ISIM simulation.

The ISIM implementation into Eulerian FCI code is enabled by the introduction of the transport quantities considering the most important melt droplet features regarding the FCI modelling. The introduced transport quantities enable an improvement of the determination of the steam explosion strength, which depends on the mass of the droplets being capable to undergo the fine fragmentation.

The potential effect of the developed ISIM approach was also assessed. The assessment was performed with an exploring version of the MC3D code. Results shows that melt solidification could importantly contribute to the observed low energy conversion efficiency in corium experiments and therefore have to be considered. Therefore, the implementation of the physically-based ISIM enhances the geometrical extrapolation capabilities of FCI codes. The capabilities of the current FCI codes could be further increased by an improved and balanced modelling of all key processes (e.g. jet fragmentation, void production, fine fragmentation).

5. Acknowledgments

The authors acknowledge the financial support of the Slovenian Research Agency within the research program P2-0026, the research project J2-2158, and the cooperative CEA-JSI research project (contract number 1000-0810-38400013). The Jožef Stefan Institute is a member of the Severe Accident Research Network of Excellence (SARNET2) within the 7th EU Framework Program.

6. References

- [1] G. Berthoud, Vapor explosions. Annual Review of Fluid Mechanics, 32, 2000, pp. 573-611.
- [2] M.L. Corradini, Vapor Explosions a Review of Experiments for Accident Analysis. Nuclear Safety, 32, 1991, pp. 337-362.
- [3] I. Huhtiniemi, H. Hohmann, D. Magallon, FCI experiments in the corium/water system. Nuclear Engineering and Design, 177, 1997, pp. 339-349.

The 14th International Topical Meeting on Nuclear Reactor Thermalhydraulics, NURETH-14 Toronto, Ontario, Canada, September 25-30, 2011

- [4] I. Huhtiniemi, D. Magallon, Insight into steam explosions with corium melts in KROTOS. Nuclear Engineering and Design, 204, 2001, pp. 391-400.
- [5] I. Huhtiniemi, D. Magallon, H. Hohmann, Results of recent KROTOS FCI tests: alumina versus corium melts. Nuclear Engineering and Design, 189, 1999, pp. 379-389.
- [6] M. Leskovar, R. Meignen, C. Brayer, M. Bürger, M. Buck, Material influence on steam explosion efficiency: state of understanding and modelling capabilities, ERMSAR, Karlsruhe, Germany, 2007.
- [7] L.A. Dombrovsky, Approximate model for break-up of solidifying melt particles due to thermal stresses in surface crust layer. International Journal of Heat and Mass Transfer, 52, 2009, pp. 582-587.
- [8] R. Meignen, D. Magallon, K.H. Bang, G. Berthoud, S. Basu, M. Buerger, M. Buck, M.L. Corradini, H. Jacobs, O. Melikhov, M. Naitoh, K. Moriyama, R. Sairanen, J.H. Song, N. Suh, T.G. Theofanous, Comparative review of FCI computer models used in the OECD-SERENA program. International Congress on Advances in Nuclear Power Plants 2005, ICAPP'05, 1, 2005, pp. 411-423.
- [9] G. Pohlner, Z. Vujic, M. Burger, G. Lohnert, Simulation of melt jet breakup and debris bed formation in water pools with IKEJET/IKEMIX. Nuclear Engineering and Design, 236, 2006, pp. 2026-2048.
- [10] M. Uršič, M. Leskovar, B. Mavko, Improved solidification influence modelling for Eulerian fuel-coolant interaction codes. Nuclear Engineering and Design, 241, 2010, pp. 1206-1216.
- [11] L.A. Dombrovsky, T.N. Dinh, The effect of thermal radiation on the solidification dynamics of metal oxide melt droplets. Nuclear Engineering and Design, 238, 2008, pp. 1421-1429.
- [12] K. Moriyama, H. Nakamura, Y. Maruyama, Analytical tool development for coarse break-up of a molten jet in a deep water pool. Nuclear Engineering and Design, 236, 2006, pp. 2010-2025.
- [13] M. Bürger, S.H. Cho, D.S. Kim, C. Carachalios, K. Müller, G. Fröhlich, Effect of solid crusts on the hydrodynamic fragmentation of melt droplets, Report. Institut für Kernenergetik und Energiesystem der Universität Stuttgart, 1985.
- [14] L.S. Nelson, P.M. Duda, Steam explosion experiments with single drops of iron oxide melted with CO₂ laser: Part II. Parametric studies, NUREG/CR 2718. Sandia National Laboratories, 1985.
- [15] S. Picchi, M. Elmo, R. Meignen, J. Lamome, MC3D Version 3.6: User's guide. IRSN, France, 2009.
- [16] M. Uršič, M. Leskovar, Solidification influence modelling in MC3D part 4: Verification and validation, Report. Jozef Stefan Institute, Ljubljana, Slovenia, 2011.